Rheology of penetrations tests II: penetrometers, Vicat and Hilti needles

D. Lootens[1], R.J. Flatt[1*], N. Roussel[2]
[1]Sika Technology AG, CH-8048 Zürich, Switzerland, [2]Laboratoire Central de Ponts et Chaussées, Paris 75732 Cedex 15, France

Abstract

In a separate paper we have shown that penetration tests mobilize the material in shear mode and that the property measured, at least in low speed tests, is yield stress [1]. However, since the critical deformation is similar for most cementitious materials, this also measures the shear modulus. Results obtained with such tests can therefore be converted to true material properties rather than remaining as the arbitrary values they are usually considered to be.

In this paper, we demonstrate this by using shear modulus measurements and comparing them to forces measured with a penetrometer for which the needle size and shape is varied. We illustrate how simple penetration experiments can be used to develop more profound analysis of cement hydration kinetics.

1 Introduction

Various empirical tests are used to follow the setting of cementitious materials. These are sometimes defined as consistency or setting time measurements. They include the Vicat needle, penetrometers and the Proctormeter also known as the Proctor needle, as well as the Hilti nail gun.

In a previous paper, we examined the situation of penetrometers in particular detail. These are instruments on which mounted needles are continuously driven into samples at a very low speed (1μm/s) while the force required to do so is measured over time. An important aspect is that the needle tip is wider than the rod on which it is mounted (Figure 1). Consequently, samples with a yield stress above a minimum value (not defined here) do not close up the gap above the tip and the surface *S* through which the needle transmits stress to the sample is constant during the experiment. A change in force over time can therefore be attributed not to a deeper penetration of the needle but to a change of the material measured.

The former paper demonstrated that the force measured is proportional yield stress. Since critical deformations in cementitious materials are relatively constant, this force is also proportional to the shear modulus.

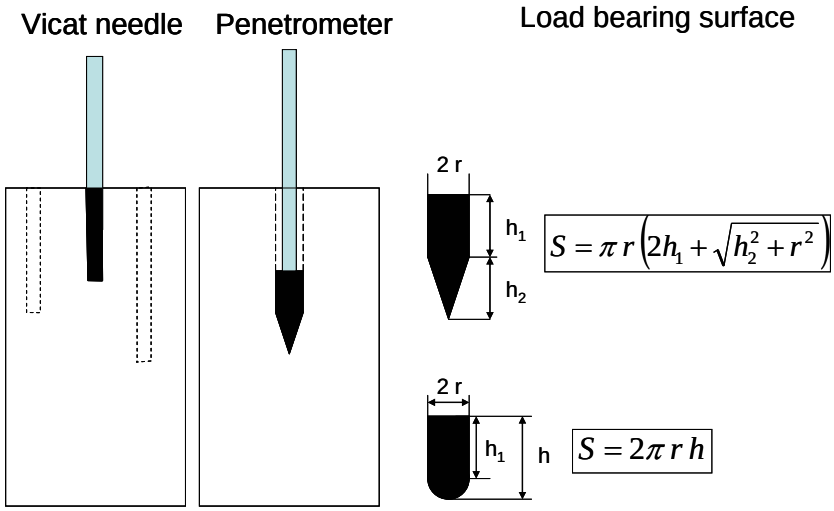

Figure 1. Schematic illustration of the difference between Vicat needle and penetrometer tests. The Vicat needle is used in different locations and the bearing surface decreases as the material stiffens (left). The penetrometer drives into the sample a needle of which the load bearing surface is constant over time (center). The expressions for those load bearing surfaces are given above for two needle geometries (right).

In this paper we vary the size and shape of the needles to demonstrate the link of such measurements to shear modulus.

2 Materials and methods

Cement pastes are prepared by adding water into a Hobart mixer already containing the cement and mixing for 2 minutes. Unless noted otherwise, no admixture is included and the W/C was 0.3. The paste is transferred into the measuring cell of a penetrometer and the needle is driven into the sample until it fully submerged. At that point the measurement is initiated, causing the sample holder to rise at 1μm/min, while the force on the needle is recorded. Several cells with different tip geometries are used in parallel to eliminate any possible variations in cement paste properties.

In addition, some material of the same type is introduced into a specially built ultrasound spectrometer operating in echo mode and with a shear transducer. Usual treatments of acoustic impedance are used to determine the shear modulus over time and data are stored on a computer. Some additional measurements were performed with a Vicat needle, using needles of different diameters.

3 Results

3.1 Hemispherical tip

Forces measured with a penetrometer having needles in the shape of hemispheres with diameters 15, 10 and 5 mm are shown in Figure 2 along with the shear modulus measured by ultrasound. A close examination of the data reveals that at long times all curves evolve as a power law of time with a similar exponent of about 5.4. A similar behaviour is also seen at short times, although in this case the exponent is unity.

These similar exponents suggest a normalisation approach where a scaling factor is used to superpose all curves onto a single one. However, cement paste is initially viscoelastic and its modulus is frequency dependent. Therefore, we normalise only for the second stage where the modulus is not frequency dependent (confirmed ultrasound measurement not reported here).

It also turns out that the forces obtained with these needles superpose extremely well when they are divided by the tip surface (Figure 3). This is consistent with Coussot's [2] prediction but differs from our FE results [1].

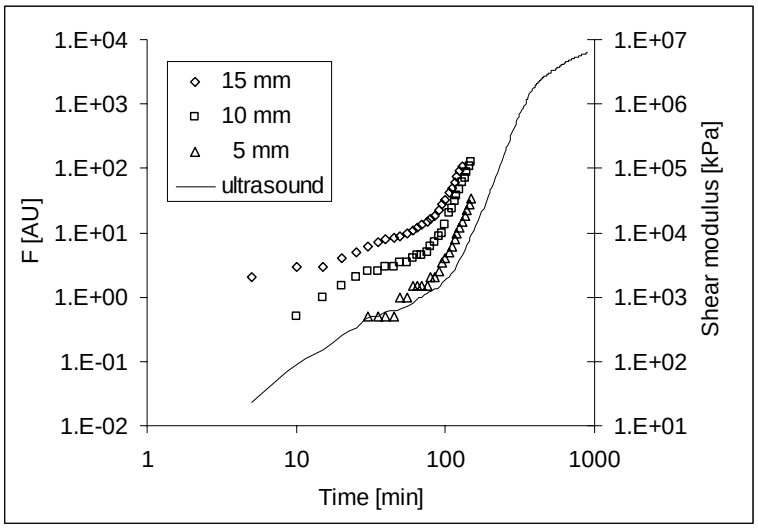

Figure 2. Shear modulus measured by ultrasound and penetration force measured with three hemispherical dips of different diameters. The scaling is such that the similar power law evolutions versus time can be seen between both types of measurements.

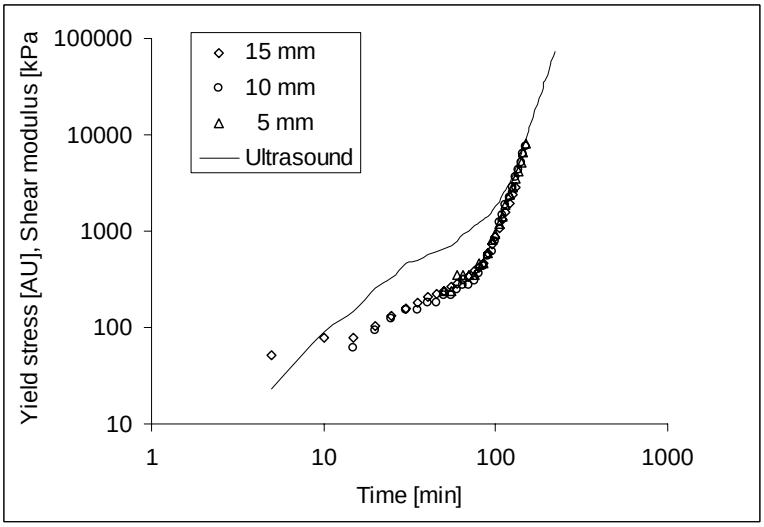

Figure 3. Ultrasound shear modulus and penetrometer force measured with hemispherical tips and normalised by the hemisphere surface. The penetrometer results are also rescaled by a single factor which collapses the data at long times on a single master curve.

3.2 Hemispherical tip and connected cylinder

As an extension to the previous tests, needles with a hemispherical end mounted on cylinders of same diameter but different lengths were used. Data for diameters of 5 and 15 mm with heights of 0, 2, 10 and 15 mm are shown in Figure 4a.

The data do not superpose well when dividing by the surface. A better superposition is however obtained if we assume that the contribution of the cylindrical part is smaller than that of the tip, and normalise by a surface analogue written as:

$$S^* = 2\pi R^2 + n_H \left(2\pi R^{2-n_H} h_1^{n_H}\right) \qquad \text{Eq. (1)}$$

In this way we are using units of surface, an approach that has also successfully been used in analysing a ball indentation penetrometer [3]. It is worth pointing out that including n_H not only as exponent but also prefactor of the second term means S^* corresponds hemispherical tip when $n_H = 0$ while as it is equal to the cylinder surface when n_H is unity.

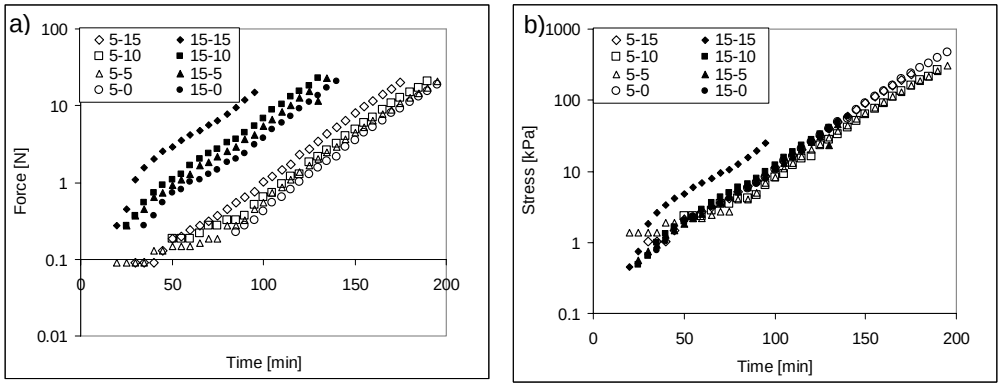

Figure 4. Penetrometer measurements with different tips. The first number in the legend is the diameter in mm of the hemispherical end and the second the height of the cylindrical section of same diameter placed above. b) uncorrected force, b) normalised by surface analogue expression given in Eq. (1).

This rather primitive surface analogue normalisation gives surprisingly good results as shown in Figure 4b. However, the data series with the largest diameter and height remain outliers. This result is reproducible and probably is a result of the needle size no more negligible compared to the cell size.

3.3 Conical tip and connected cylinder

In a series of experiments with conical tips, we use an expression analogous to Eq. (1) adapted for a conical rather than a hemispherical end:

$$S^* = \pi R\sqrt{R^2 + h_2^2} + n_H \left(2\pi R^{2-n_H} h_1^{n_H}\right) \qquad \text{Eq. (2)}$$

where h_1 and h_2 are the high of the cylindrical and conical section respectively (Figure 1).

However, in this case the best superposition is obtained when n_H is unity, so that we are dividing by the needle surface (Figure 5). The contribution of the cylindrical section therefore seems to be influenced by the tip shape. It

is not clear why this should be the case, but it is important to underline the difference.

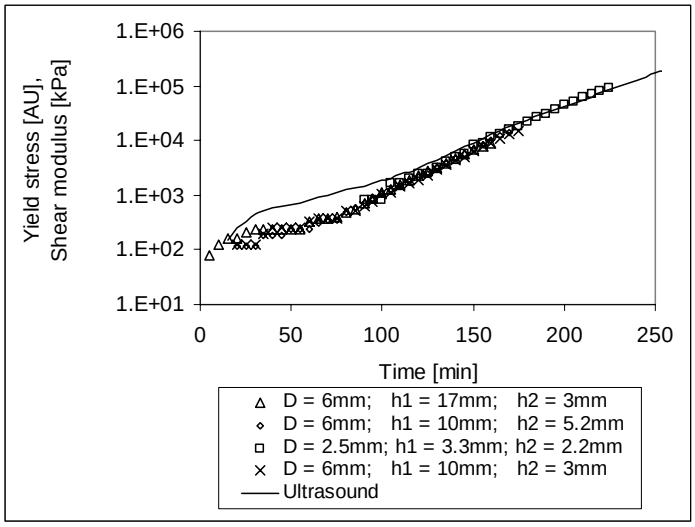

Figure 5. Pentrometer force normalised by surface of conical tip.

3.4 Vicat needle

Measurements with the Vicat needle, using two diameters of the needle are found to be comparable using similar surface equivalent approach but neglecting the end surface. In this case, the value of n_H is found to be 1.2.

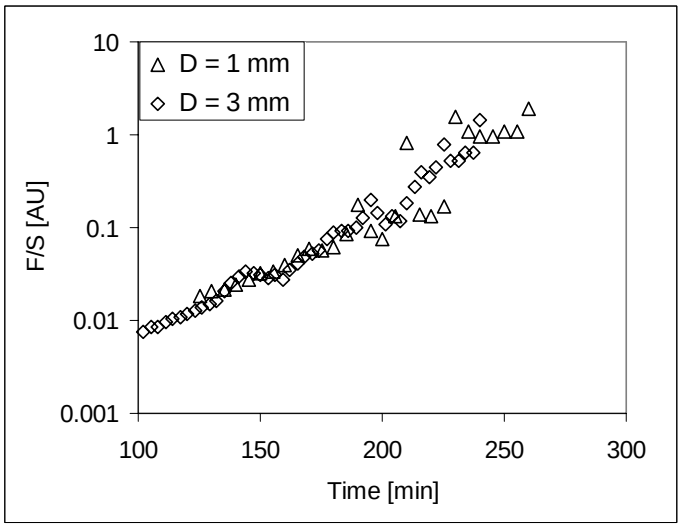

Figure 6. Vicat test where the fixed load is normalised by an equivalent surface where the radius exponent is 0.8 and the penetration depth exponent is 1.2.

4 Discussion

4.1 Basic concepts

The results presented for the hemisphere tip show that data correlate with the shear modulus at long times. They also show similar evolution at shorted times but with a scaling factor that depends on the viscoelastic nature of the material over that period of time.

Data obtained using a hemispherical tip can be well normalised by dividing by the hemisphere radius. Thus we find a force that scales with the second power of radius rather than its 2/3 as found in [1]. As mentioned in that article such a result may be explained in the following way [4]. First it is assumed that Stokes law can be used:

$$F = 6\pi\eta RV \qquad \text{Eq. (3)}$$

where η is the viscosity of the continuous phase, *R* is the sphere radius and *V* its velocity.

If the material can be assumed to have a Bingham type behaviour then we have:

$$\tau = \tau_0 + \eta_B \dot{\gamma} \qquad \text{Eq. (4)}$$

where τ_0 is the yield stress and η_B the plastic viscosity. Substitution into Eq. (3) gives:

$$F = 6\pi R\left(\frac{\tau_0}{\dot{\gamma}} + \eta_B\right)V \qquad \text{Eq. (5)}$$

For a quasi-static condition, we do not have to worry about η_B but only about $\tau_0/\dot{\gamma}$. Furthermore for a sphere, it has been shown that the velocity gradient is well approximated by [5]:

$$V \cong k\dot{\gamma}/(2R) \qquad \text{Eq. (6)}$$

where *k* is a constant close to unity. Substitution into Eq. (3) gives

$$F = 12\pi R^2\tau_0 \qquad \text{Eq. (7)}$$

This would imply that the force would be equal to 6 times the product of the surface by the yield stress. The proportionality factor between force and elastic modulus is similar (5.1), implying that the critical strain is unity which is not consistent with what is known for cementitious systems [6].

An alternative approach is to assume that the load is carried by needle surface. This leads to underestimating the load while as above it is overestimated. The reason is that the interface between the elastic and plastic zone which is not located at the tip surface even at low speed [1, 7].

4.2 Tip size and shape

In the case of the hemispherical tip, data normalise well with R^2, as suggested above. However, when the hemispherical tip is extended with a cylinder of same diameter and varying height, we find that Eq. (1) leads to a good normalisation with values of n_H of 0.5.

On the other hand, needles having conical tips lead to data that normalise well with their surfaces (n_H is equal to 1 in Eq. (2)). This suggests that the force on the cylindrical section scale differently according to the shape of the needle end. This possibility will be discussed below in the analysis of the Hilti and Vicat needle tests.

4.3 Hilti needle

In the Hilti needle test, a needle is shot into a cementitious material and the penetration depth is taken as indicative of strength. Data are generally analysed in terms of the Bracher table. This relates compressive strength to penetration depth through the following exponential function (continuous line in Figure 7).

$$C_S = C_{S_0} + C_{S_1} \exp\left(-\frac{P}{P_0}\right) \qquad \text{Eq. (8)}$$

where $C_{S_0} = 5\,10^3\ Pa$, $C_{S_1} = 6\,10^7\ Pa$ and $P_0 = 25.7\ mm$.

However, as indicated in Figure 7 an inverse 2nd power of penetration depth fits the data very well.

For this type of test, we consider that the needle is given a certain energy and that it stops once the energy has been fully dissipated. In this case the role of plastic viscosity is most probably not negligible. If nevertheless, we neglect it for convenience, the dissipated energy can be written as:

$$U \cong \int_0^H F\,dH \approx \tau_0 R^{2-n_H} \int_0^H h^{n_H}\,dh \approx \tau_0 R^{2-n_H} H^{n_H+1} \qquad \text{Eq. (9)}$$

where the shape of the needle end may affect the value of n_H, although its contribution to the loaded surface is neglected. This is also written as:

$$\tau_0 \approx \frac{1}{R^{2-n_H} H^{n_H+1}} \qquad \text{Eq. (10)}$$

Thus the result in Figure 7 may be understood if compressive strength scales with the shear yield stress and if n_H is unity as in the case of the cone tips rather than the hemispherical ones. Since the nails use are in have conical ends, this result is quite consistent.

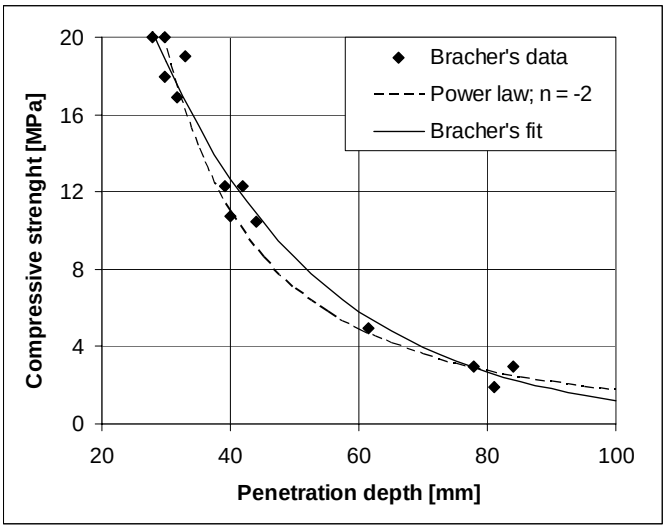

Figure 7. Hilti needle data from Bracher. The continuous line corresponds to Eq. (8), while the discontinuous line is an inverse second power fit.

4.4 Vicat needle

The Vicat needle may be thought of in a similar way as the Hilti needle. However, in this case, the energy available is a potential energy due to gravity. The dissipated energy is thus proportional to the depth to which the sample penetrates. Alternatively, we can consider that at stoppage, the needle load is carried by the surface of the plastic-elastic interface and use a similar analogous surface expression to Eq. (1) or Eq. (2), but in which the first term is neglected. In both cases we then get:

$$\tau_0 \approx \frac{mg}{R^{2-n_H} H^{n_H}} \qquad \text{Eq. (11)}$$

We find that a value of 1.2 for n_H allows a good superposition of the data, but more extensive tests would be needed to check this result.

4.5 Hydration kinetics

The above results point to the fact that penetration techniques scale with the shear yield stress of the material. Thus, with a continuously measuring instrument as a penetrometer, the force measured should be directly proportional to the yield stress or elastic modulus. We saw that such data appears well represented by two stages that can be fit by power laws.

Here we take this analysis a step further. We average the normalised penetrometer results and examine the type of functions that describe their evolution best.

A condition which is found to fit such data well is to assume that in a first stage there is a stiffening of the matrix which follows a hyperbole function. In this way the matrix properties are constant at long times and increase linearly at short ones. This process may be though more of as a flocculation stage. We then assume that the more massive precipitation of hydrates in the acceleration period increases the volume of solid inclusions in that matrix. In this way a material property as shear modulus is the product between the value of that property for the matrix and a function of volume fraction of inclusions. If the increase in volume fraction of inclusions follows a power law of time we then describe the features observed on our data (until the slowing down stage).

$$G = \frac{G_{floc}^{\max} t}{G_{floc}^{\max} / \alpha + t}\left(1 + \beta\, t^{n}\right) \qquad \text{Eq. (12)}$$

where $G_{floc}^{\max}$ is the shear modulus of the flocculated network at infinite time, α is the slope describing modulus increase at short time, β is the prefactor of the power law describing the acceleration period behaviour and *n* is the exponent of the power law (5.4 for these samples),

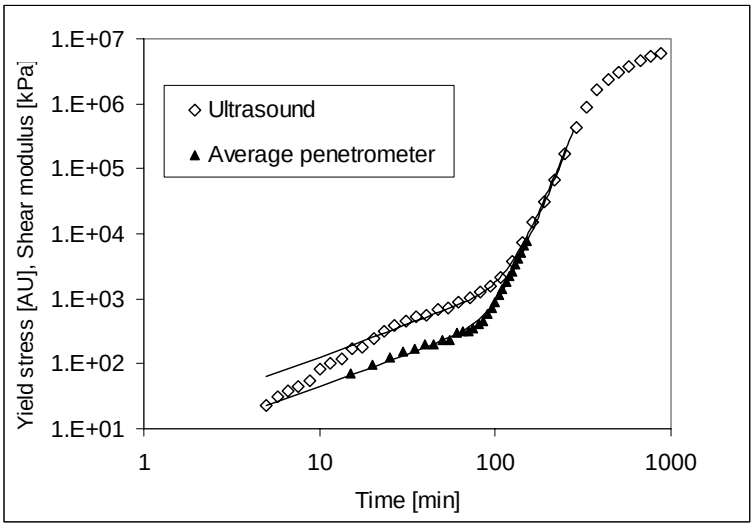

Figure 8. Ultrasound shear modulus and average of normalised penetrometer forces measured with hemispherical tips. The continuous lines show the proposed fitting curves in Eq. (4). The ultrasound data has been reduced for the purpose of illustration.

A possible interpretation of the exponent value is as follows. For gels, it is established the Young's modulus is a power law of density with an exponent of about between 2.6 and 3.7 regardless of the microstructural and chemical differences [8]. In the zone we are considering the Poisson ratio is constant and the evolution of the shear and Young modulus are parallel. It should be noted that the range of exponents reported by Ma [9],

is similar to what has been reported for the yield stress of suspension [10]. In that case, for low values of the percolation threshold, the dependence of yield stress on volume fraction ϕ is expressed as $\phi^3/(\phi^*-\phi)$, where ϕ^* is the geometrical maximum packing. The exponent of the numerator is obtained by considering the number of contacts and the fact that the stress is transmitted through the solid network. In the case we consider, stress may also be transmitted through the matrix, so that an exponent of 2 rather than 3 would be more appropriate. If furthermore the volume fraction is not too close to the maximum packing, then we expect a scaling of yield stress with the second power of modulus. A similar reasoning for the gels would lead to assuming that the scaling factors reported by Ma for the elastic modulus of gels would lie rather between 1.6 and 2.7 if the stress can also be transmitted through the matrix.

Furthermore, among the various expressions used to quantify the kinetics of the acceleration period, some authors report a power law evolution with an exponent of about 2.5 [11] (A similar value is obtained (3) when the Avrami equation is used with an exponent of 3, as reporeted by Grartner et al [12]). Combining both results would suggest a power law increase of modulus with time with an exponent between 4 and 6.75, which is in the range observed with our high tech penetrometers. Further investigations are however necessary to determine the extent to which these simple considerations really capture key processes in cement hydration.

Apart from this, it is worth noting that a simpler expression than Eq. (12) may be used. It has the advantage of reducing the number of fitting parameters from 4 to three per curve. Indeed, the asymptote not being reached for the first stage phenomena, we can approximate the function by:

$$G = \alpha^* \, G_{floc}^{\max} t \left(1 + \beta^* \, t^{n^*}\right) \qquad \text{Eq. (13)}$$

where α^*, β^* and n^* have similar meaning to α, β and n^* previously.

It should be noted the ultrasound and normalised penetrometer data share the values of β^* and n^*. Taking into account the normalisation factor this means that 5 parameters are needed to fit both data series. The resulting fit is pretty good as indicated in *Figure 8*.

5 Conclusions

Systematic variations in the tip geometries of a penetrometer needle have made it possible to confirm experimentally that such measurements are linked to the shear properties (modulus and yield stress) of cementitious materials.

In the case of a hemispherical tip, the forces scale with the tip radius. The

situation is however more complex with different geometries and additional work would be needed to confirm the proposed scaling relations.

When used correctly, a penetration technique provides a measurement that is proportional to a real material property and is therefore not as empirical as generally assumed.

6 References

[1] P. Jousset, D. Lootens and R.J. Flatt, Rheology of penetrations tests I: theory and finite element simulations, 12th ICCC, Montreal (2006).

[2] P. COUSSOT. Rheometry of Pastes, suspensions and granular materials: Applications in Industry. J Wiley & Sons, 2005, ch. 7, pp. 246–253.

[3] L.L. Chapoy and J.J. Aklonis, “The desing and calibration of a stress relaxation ball indentation penetrometer”, Trans. Soc. Rheol. 13:3, 445-455 (1968).

[4] N. Roussel, “A theoretical frame to study stability of fresh concrete”, RILEM Materials and Structures, Vol. 39(1), pp. 75-83, 2006.

[5] Ansley, R.W. and Smith, T.N, “Motion of spherical particles in a Bingham plastic”, *A.I.Ch.E. Journal* 13 (1967) 1193-1196.

[6] L. Nachbaur , J.C. Mutin, A. Nonat and L. Choplin, “Dynamic mode rheology of cement and tricalcium silicate pastes from mixing to setting“, Cem Concr Res 31 (2001) 183-192.

[7] Hill, R., , “The mathematical theory of plasticity” (Oxford University Press), Oxford (1950).

[8] H.-S. Ma “Aggregation-Structure-Elasticity Relationship of Gels“, PhD thesis, Princeton University (2002), see Table 2 in Chapter 2.

[9] H.-S. Ma “Aggregation-Structure-Elasticity Relationship of Gels“, PhD thesis, Princeton University (2002), see Table 2 in Chapter 2.

[10] Flatt R.J., Bowen P., “YODEL: a Yield stress mODEL for suspensions”, J. Am. Ceram. Soc. 89 [4] (2006) 1244-1256.

[11] F. Tschichholz and H. Zanni, “Global hydration kinetics of tricalcium silicate cement“, Phs. Rev. E., 64 (2001) 016115.

[12] E.M. Gartner, J.F. Young, D.A. Damidot and I. Jawed, “Hydration of Portland Cement”, in “Structure and Performance of Cements” (Eds. J. Bensted and P. Barnes), Spon Press, London, 2002, pp. 57-113.